Refraction and Reflection of Diffusion Fronts

A. Remhof,* R. J. Wijngaarden, and R. Griessen

Faculty of Sciences, Division of Physics and Astronomy, Vrije Universiteit, De Boelelaan 1081,
1081 HV Amsterdam, The Netherlands

Diffusion waves form the basis of several measurement technologies in materials science as well as in biological systems. They are, however, so heavily damped that their observation is a real challenge to the experimentalist. We show that accurate information about the refractionlike and reflectionlike behavior of diffusion *waves* can be obtained by studying diffusion *fronts*. For this we use hydrogen in a metal as a model system and visualize its 2D migration with an optical indicator. The similarities between classical optics and diffusion, in particular, the applicability of Snell's law to diffusive systems are discussed. Our measurements are in good agreement with numerical simulations.

Generally, a wave can be defined as a propagating imbalance. This imbalance may be the density fluctuation in an elastic medium that leads to acoustic waves. In the case of linear restoring forces, such as in an elastic medium, there is a periodic conversion of different forms of energy. In contrast, an imbalance in concentration does not lead to a concentration wave due to the lack of a restoring force. Such a system does not *overshoot* its equilibrium concentration and does not form a self-sustained concentration wave. Therefore, concentration waves occur only as a result of locally imposed forced oscillations. Forced oscillations of particles or energy in a diffusive medium are known as *diffusion waves*. Mathematically, they are solutions of the diffusion equation

$$\frac{\partial c}{\partial t} = D \Delta c, \qquad (1)$$

where D denotes the diffusivity of the medium in which the concentration $c(\vec{r}, t)$ is forced to vary as $\sin(\omega t)$ in a chosen region of the sample. Examples are the temperature profile of Earth resulting from the seasonal temperature variation [1] or diffuse photon density waves in turbid media [2]. Similar behavior is observed in reaction-diffusion systems that are described by more complex differential equations than diffusion [3,4]. Diffusion waves form the basis of numerous measurement techniques in materials science as well as in optical mammography. Reviews on diffusion waves together with examples of their technological applications have been published by Yodh [5] and by Mandelis [6]. A characteristic feature of diffusion waves is the strong damping which makes the investigation of diffusion waves quite challenging. In what follows, we show that the behavior of diffusion fronts, which are relatively easy to generate and to monitor, is closely related to the behavior of the often elusive diffusion waves.

In general, a simple model system to study the behavior of diffusion fronts and waves consists of two adjacent media with different diffusivities. A constant or an oscillatory source of particles or energy placed close to the interface produces spherical isoconcentration lines or spherical diffusion waves that become distorted as they cross the interface. Mandelis [7] and Shendeleva [8] recently carried out extensive theoretical studies of parabolic diffusion wave fields at linear and planar interfaces and discussed the validity of refraction and reflection concepts for diffusion waves. Experimentally, this problem has been studied so far for photon density waves in turbid media [2]. The behavior of the diffusion wave could not, however, be studied with sufficient accuracy to discuss quantitatively the validity of Snell's law.

The purpose of this work is to consider a simple purely diffusive system that allows detailed and accurate measurements of the influence of a boundary on diffusing particles. For this we choose the fast diffusion of hydrogen in thin vanadium (V) layers. A thin Y cap layer is used for two purposes: (i) as an agent to control the effective H diffusivity of the sample and (ii) as an optical indicator, where the different colors of YH_x allow one to visualize the diffusion process [9,10]. The diffusion constant D of H in V is much larger than in Y. Additionally, the enthalpy of hydrogen solution in Y is much more negative than in V; in other words, the hydrogen affinity of Y is much larger than the hydrogen affinity of V. Consequently, in a lateral diffusion experiment in Y/V bilayers, most hydrogen flows via the V into the Y. The occurrence of stable hydride phases in the Y/H system [11] separated by large miscibility gaps results in sharp, well defined diffusion fronts. The front separating the saturated α phase (H/Y = 0.2) from the β phase (H/Y = 1.9) is experimentally found to move as $x_f^2 = Kt$. The front mobility K is high for a thick V layer offering a large cross section for the H supply and for a thin Y layer that is quickly H saturated. In other words, Y/V bilayers represent a two-dimensional solid-state system in which the effective H mobility is varied locally by the Y/V thickness ratio [12]. In the Y/V bilayers the Y also plays the role of an optical H indicator.

The samples are prepared by electron beam evaporation at ultrahigh vacuum conditions. A detailed description of the sample preparation is given in Ref. [12]. The deposition process (thickness, growth rate) is monitored *in situ* by means of a water cooled quartz microbalance. Prior to hydrogenation, the sample thickness is measured *ex situ* by profilometry and by Rutherford backscattering (RBS). Furthermore, the RBS spectra show well defined layers, no intermixing at the interfaces, and no chemical contaminations. The thickness of the natural oxide layer formed in ambient air on the uncovered part of the yttrium layer is determined to be 15 nm. In the sample design shown in Fig. 1, the intrinsic H concentration-dependent optical properties of the Y cap layer [9] are exploited for the visualization of the lateral migration of hydrogen [10]. The Pd dot serves as a gate to the surrounding H reservoir. The passivating Y_2O_3 layer that forms in ambient air on the Pd-free parts of the sample blocks direct hydrogenation of other parts of the sample. The gas phase loading of the samples is carried out in the same experimental setup as used by den Broeder *et al.* [10]. The gas loading cell together with the imaging system has been described recently [13]. Figure 2 depicts a sequence of four images, recorded in reflection mode during hydrogen loading. The sample is kept at 373 K. At $t = 0$ the sample is exposed to a hydrogen atmosphere of $p_{H_2} = 10^5$ Pa. The Pd dot can be recognized as the bright spot in the lower half of the photographs.

Immediately after hydrogen exposure, the Y/V bilayer underneath the Pd starts absorbing hydrogen and saturation is reached within seconds. The H concentration in the Y layer, serving as optical H indicator, decreases from $c_H = 2.7H/Y$ in the trihydride phase below the bright, shiny metallic Pd dot to essentially $c_H = 0$ far away from it. The resulting concentration gradient is the driving force for the lateral diffusion. Further hydrogen uptake is now achieved by fast H diffusion mainly through V. The front separating the shiny metallic hydrogen-free part of the sample from the darker, hydrogen-loaded

part of the sample is the most noticeable optical feature of the system. The radius r_f of the circular front expands initially as $r_f^2 = Kt$, where $K_1 = 4.1 \times 10^{-6}$ cm^2/s. As soon as the front reaches the high diffusivity medium, it bulges out and a mushroom-shaped pattern is formed. This behavior of the diffusion front reminds us of a classical optical wave front that propagates into a medium with a lower index of refraction. This similarity suggests the construction of diffusion rays in the following way: The starting point of the ray is chosen at the center of the Pd disk. This ray intersects the boundary between the two media at an angle θ_1 with respect to the normal. After this intersection, the direction of the straight *refracted* ray is perpendicular to the diffusion front and makes an angle θ_2 with the normal. In classical optics *rays* in the above-mentioned way accurately describes the propagation of light at an interface separating two adjacent isotropic media. They are a consequence of Fermat's principle. We show experimentally and in numerical simulations that this concept, despite certain similarities, is not applicable to a diffusive system in which the propagation of particles is driven by the gradient of the chemical potential.

Similarly to O'Leary's detailed study of the refraction-like behavior of photon density waves in turbid media [2],
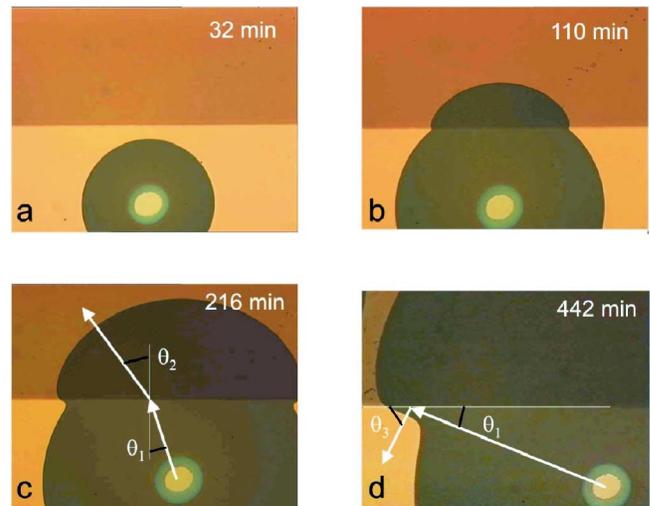
FIG. 2 (color online). Temporal evolution of the hydrogen front in the sample of Fig. 1. Each image depicts a 5.6×4.5 mm^2 large area of the sample. All images are recorded in reflection, in a hydrogen atmosphere of 10^5 Pa at 373 K. In the upper half of the sample, the V layer is 250 nm thick; in the lower half, its thickness is 50 nm. The Pd dot is in the lower half of the sample, 1.5 mm away from the interface. The hydrogen diffusion starting from the Pd dot can be followed via the formation of dark YH_2 in the Y indicator. Close to the dot, the bright H-rich YH_3 phase forms. Note the deformation of the formerly circular diffusion front (a) as it crosses the interface (b)–(d). In panels (c) and (d) we show two diffusion rays to discuss the applicability of Snell's law and the concept of total reflection, respectively (see text).
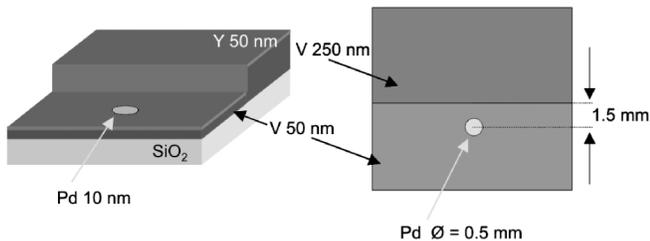

FIG. 1. Schematic sample design. A stepped V film with respective thicknesses of 50 and 250 nm, covered completely with 50 nm Y, is deposited on an amorphous quartz substrate. To confine the H loading a 0.5 mm large, 10 nm thick Pd dot is deposited 1.5 mm away from the interface separating the areas of different thickness. The figure on the left gives a perspective view of the sample; the figure on the right gives a top view.

we observe within experimental error that Snell's law accurately describes the *refraction* of the H-diffusion front at small angles, where $\sqrt{K}$ plays the role of the refractive index. Near the critical angle of $\theta_1 = 26°$, where $\sin\theta_2$ approaches unity, the *refracted* diffusion front becomes heavily distorted, indicating that Snell's law is violated. Our experiment has, however, the great advantage that we can observe the temporal development of a sharp, well defined isoconcentration line, including the distorted area close to the interface. There is also a more fundamental difference with photons in a turbid medium: Hydrogen does not suffer from absorption; therefore, particle loss does not occur. In a theoretical study of the refraction of a transient temperature field at a plane interface based on the Cagniard–de Hoop technique, Shendeleva [8] pointed out that the *rays* as constructed above do not represent the direction of particle flux in the medium. The particle flux $\vec{J}$ follows from the gradient in concentration

$$\vec{J} = -D\nabla c, \tag{2}$$

where D is the diffusion coefficient and c denotes the hydrogen concentration. The magnitude and direction of $\vec{J}$ varies spatially and temporally. This is clearly at variance with optics in which the velocity of light depends on a scalar quantity, the refractive index. This is not the case for diffusion and the particle flux is not expected to obey Snell's law.

Apart from the refractionlike behavior of near-normal incidence *rays,* we also observe a reflectionlike behavior at the interface. However, tracing a *reflected* ray back to the source in the same way as we constructed the *refracted* ray [see Fig. 2(d)], it is apparent that the usual reflection law $\theta_1 = \theta_3$ does not apply at all. That a *reflectionlike* behavior nevertheless occurs is due to particles diffusing from the slower half of the sample through the faster diffusive medium back into the slow medium. This bypassing results in an accumulation of H atoms along the interface. The resulting accumulation has been discussed theoretically [7] and the back diffusion was also found in certain reaction-diffusion systems [3].

We compare now our experimental results with numerical simulations where the equations (1) and (2) are solved with a finite element technique. The only input parameters are the two different diffusivities and the hydrogen concentration below the Pd dot. At the start of the simulation the concentration is zero everywhere. We simulate the following two situations:

(i) A diffusion wave with a sinusoidal oscillatory source term at the Pd dot. In Fig. 3 we plot the phase difference between the source and the foremost zero crossing of the concentration. Identical colors represent identical phase (modulo 2π). The lines of constant phase thus represent also low concentration isoconcentration lines. These calculated lines reproduce the low concen-
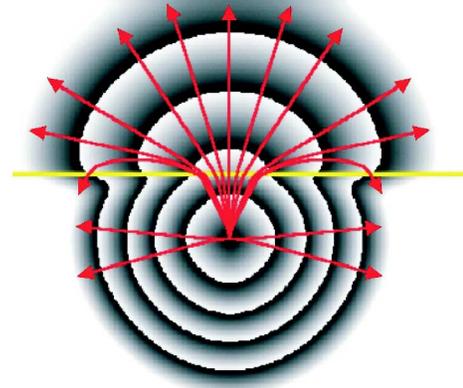

FIG. 3 (color online). Calculated 2D diffusion wave field. The wave is excited from a point source $c(0, t) = \sin(\omega t)$. Superimposed are some representative flux lines. Note the refractionlike and reflectionlike phenomena at the interface separating two half planes with different diffusivities.

tration isoconcentration line monitored in our experiment. At each point the gradient of the concentration is calculated as well. Some of the corresponding flux lines are superimposed to the wave field in Fig. 3. In Fig. 4 a detail of Fig. 3 with calculated flux lines near the interface is shown. Above a critical angle, a total reflectionlike regime is observed, where all flux lines merge. The resulting particle accumulation leads to increased front speed. The merging of all reflected lines, where the angle of reflection is always equal to the critical angle, was previously also found for chemical waves [4].

(ii) A stepwise increase in H concentration at the Pd dot at $t = 0$ from $c = 0$ to c_0. The resulting low concentration isoconcentration lines reproduce the isophase lines of the first simulation and also the experimentally observed mushroom-shaped diffusion front.

The agreement between the observed diffusion front and the calculated lines of constant phase in the diffusion wave simulation (i) and with the calculated isoconcentration line in simulation (ii) is not trivial. It is observed only for low isoconcentration lines. This implies that, if in an experiment one is able to detect a diffusion front corresponding to a very low concentration, the behavior of this front will be the same as the behavior of constant phase
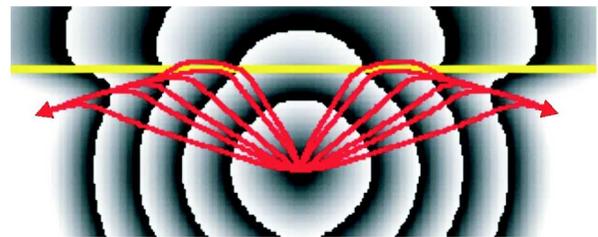

FIG. 4 (color online). Detail of Fig. 3 to show the reflectionlike behavior of flux lines. In contrast to optics, there is an accumulation of flux lines in diffusion.

lines in a diffusion wave. This can be advantageously exploited in designing experiments.

Another possibility to facilitate the study of diffusion waves is provided by the fact that H in a metal has a nonzero effective charge. In the presence of a constant electric field $\vec{E}$, the H ion experiences a force parallel to the electric field, leading to *electrodiffusion* waves that are solutions of the following modified diffusion equation [14] with D constant:

$$\frac{\partial c}{\partial t} = D\Delta c - D\frac{\partial}{\partial c}\left[\frac{eZ}{\partial\mu/\partial c}\right]\vec{E}\cdot\nabla c, \qquad (3)$$

where eZ denotes the effective charge of the H ion, and μ is its chemical potential in the host metal. The factor in the linear term of Eq. (3)

$$\vec{v}(c) = D\frac{\partial}{\partial c}\left[\frac{eZ}{\partial\mu/\partial c}\right]\vec{E} \qquad (4)$$

has the dimension of a velocity. In contrast to diffusion waves, electrodiffusion waves have the great advantage to exist at all frequencies and to suffer much less from damping.

In conclusion, we demonstrated that: (i) the visualization of H migration with switchable mirrors offers a very accurate means to study the behavior of diffusion fronts at interfaces, (ii) the theoretical concepts developed to describe the refractionlike and reflectionlike behavior of heat flow at planar interfaces apply also to diffusing particles, (iii) the refractionlike behavior is similar to its optical analogon since Snell's law holds for incident angles up to the critical angle of 26°, (iv) the reflectionlike behavior is totally different from its optical analogon but very much like the behavior of reaction-diffusion systems, since all the reflected beams do eventually merge together, and (v) diffusion fronts corresponding to very small concentrations have the same behavior as lines of constant phase in diffusion waves. This is of practical significance since concentration step experiments are much simpler to perform than oscillatory experiments (i.e., diffusion waves). In this way, H diffusion could be used as a model system for diffusion wave propagation in diffusive systems, for example, for light in turbid media (mammography). The absorption of photons occurring in such a system can be mimicked in our system with an H absorbing layer of desired thickness, since this layer continuously sucks H away from the system under investigation.

---

*Present address: Institut für Experimentalphysik/ Festkörperphysik, Fakultät für Physik und Astronomie, Ruhr-Universität Bochum, 44780 Bochum, Germany. Electronic address: arndt.remhof@ruhr-uni-bochum.de

[1] A. Sommerfeld, *Partielle Differentialgleichungen der Physik* (Verlag Harri Deutsch, Thun, 1978), reprint of 6th ed.

[2] M. A. O'Leary, D. A. Boas, B. Chance, and A. G. Yodh, Phys. Rev. Lett. **69**, 2658 (1992).

[3] A. M. Zhabotinsky, M. D. Eager, and I. R. Epstein, Phys. Rev. Lett. **71**, 1526 (1993).

[4] J. Sainhas and R. Dilão, Phys. Rev. Lett. **80**, 5216 (1998).

[5] A. Yodh and B. Chance, Phys. Today **48**, No. 03, 34 (1995).

[6] A. Mandelis, Phys. Today **53**, No. 08, 29 (2000), and references therein.

[7] A. Mandelis, L. Nicolaides, and Y. Chen, Phys. Rev. Lett. **87**, 020801 (2001).

[8] M. L. Shendeleva, Phys. Rev. B **65**, 134209 (2002); M. L. Shendeleva, J. Appl. Phys. **91**, 3444 (2002); M. L. Shendeleva, J. A. Molloy, and N. N. Ljepojevic, Appl. Phys. Lett. **80**, 1486 (2002); M. L. Shendeleva, Phys. Rev. E **64**, 036612 (2001).

[9] M. Kremers, N. J. Koeman, R. Griessen, P. H. L. Notten, R. Tolboom, P. J. Kelly, and P. A. Duine, Phys. Rev. B **57**, 4943 (1998).

[10] F. J. A. den Broeder, S. J. van der Molen, M. Kremers, J. N. Huiberts, D. G. Nagengast, A. T. M. van Gogh, W. H. Huisman, N. J. Koeman, B. Dam, J. H. Rector, S. Plota, M. Haaksma, R. M. N. Hanzen, R. M. Jungblut, P. A. Duine, and R. Griessen, Nature (London) **394**, 656 (1998).

[11] P. Vadja, in *Handbook on the Physics and Chemistry of Rare Earths*, edited by K. A. Gschneidner and L. Eyring (Elsevier, Amsterdam, 1995), Vol. 20.

[12] A. Remhof, S. J. van der Molen, A. Antosik, A. Dobrowolska, N. J. Koeman, and R. Griessen, Phys. Rev. B **66**, (R)020101 (2002).

[13] A. Remhof, J. W. J. Kerssemakers, S. J. van der Molen, E. S. Kooij, and R. Griessen, Phys. Rev. B **65**, 054110 (2002).

[14] S. J. van der Molen, M. S. Welling, and R. Griessen, Phys. Rev. Lett. **85**, 3882 (2000).